

TR-76-4

ADA023190

ANALYSIS OF NONLINEARLY LOADED N-PORT ANTENNA STRUCTURES

by

Jagan K. Sarkar  
Donald D. Weiner  
Roger F. Harrington

Department of  
Electrical and Computer Engineering  
Syracuse University  
Syracuse, New York 13210

Technical Report No. 2

April 1976

Contract No. N00014-76-C-0225

Approved for public release; distribution unlimited.

Reproduction in whole or in part permitted for any  
purpose of the United States Government.

Prepared for

DEPARTMENT OF THE NAVY  
OFFICE OF NAVAL RESEARCH  
ARLINGTON, VIRGINIA 22217





**20. Abstract (cont'd.)**

technique. A procedure for obtaining a time domain solution from the frequency domain solution without using fast Fourier transform techniques is demonstrated.



## CONTENTS

	Page
1. INTRODUCTION-----	1
2. VOLTERRA SERIES ANALYSIS-----	2
3. MULTIPLE INPUT VOLTERRA SERIES-----	6
4. DETERMINATION OF THE NONLINEAR TRANSFER FUNCTION-----	8
5. APPLICATION OF VOLTERRA SERIES TO A NONLINEARLY LOADED ANTENNA STRUCTURE-----	23
6. RESULTS-----	27
7. IMPLICATIONS OF THE RESULT-----	31
8. CONCLUSION-----	33
9. REFERENCES-----	34

ACCESSION for		
RTIS	White Section	<input checked="" type="checkbox"/>
DJB	Buff Section	<input type="checkbox"/>
UNANNOUNCED		<input type="checkbox"/>
JUSTIFICATION.....		
BY.....		
DISTRIBUTION/AVAILABILITY CODES		
Dist.	AVAIL. and/or SPECIAL	
A		

## 1. INTRODUCTION

The Volterra series [1] analysis of nonlinear systems with memory was introduced by Wiener [2] and later applied by Van Trees [3] in the analysis of nonlinear feedback systems and by Bedrosian and Rice [4] in the analysis of nonlinear distortion in communication devices. Weiner and Naditch [5] employed scattering variables to extend the Volterra technique to high frequency systems, including those containing linear distributed component devices. Recently Sarkar and Weiner [6] applied the Volterra technique to the analysis of nonlinearly loaded antennas. As demonstrated by them, the response at any intermodulation frequency is obtained by solution of the linearized equivalent network in which the nonlinearities appear as known excitations. This approach differs from conventional time-domain solutions in that individual frequency components in the output can be determined directly without the need to perform a fast Fourier transform on the total time-domain solution [7] or to go through the tedious process of searching for poles in the complex frequency plane [8]. This is an important advantage when frequency components of interest are of small magnitude compared to the total waveform. The computations made by Sarkar and Weiner [6] agreed with the experimental results for responses at different power levels and scattered frequencies.

The objective of this paper is to extend the formulation [6] to nonlinearly loaded N-port structures. This may be utilized to solve a nonlinearly-loaded multiport antenna structure situated over an imperfect ground plane. Recently, user-oriented computer programs [9-15] have been developed to analyze an antenna structure over an imperfect ground plane using both the Sommerfeld formulation and the reflection coefficient method

Both of the above mentioned solution procedures may be utilized to analyze an arbitrarily oriented multiply-nonlinearily loaded antenna structure over a plane surface of a homogeneous isotropic earth.

## 2. VOLTERRA SERIES ANALYSIS

The Volterra approach assumes that the response of a nonlinear system, having input  $x(t)$  and output  $y(t)$ , can be expressed as

$$y(t) = \sum_{n=1}^{\infty} y_n(t) \quad (2.1)$$

where  $y_n(t)$  is the  $n$ th order portion of the response and is given by

$$y_n(t) = \int \int \dots \int h_n(\tau_1, \dots, \tau_n) \prod_{p=1}^n x(t - \tau_p) d\tau_p \quad (2.2)$$

The symbol  $\int$  denotes an  $n$ -fold integration from  $-\infty$  to  $+\infty$  while  $\prod_{p=1}^n$  denotes an  $n$ -fold product.  $y_n(t)$  is of  $n$ th order in the sense that multiplication of the input  $x(t)$  by constant  $A$  results in multiplication of  $y_n(t)$  by  $A^n$ . Systems having Volterra functional representations are referred to as "Volterra Systems."

In practice, the Volterra approach is most useful when the response  $y(t)$  can be adequately approximated by a finite number of terms. This is the situation commonly encountered in soft nonlinearities where the nonlinear distortions may be 20 dB or more below the input signals. In this paper it is assumed that all responses are adequately characterized by the finite sum

$$y(t) = \sum_{n=1}^N \int \int \dots \int h_n(\tau_1, \dots, \tau_n) \prod_{p=1}^n x(t - \tau_p) d\tau_p \quad (2.3)$$

The  $n$ th order Volterra kernel  $h_n(\tau_1, \dots, \tau_n)$  is referred to as the  $n$ th order impulse response. In actuality, the impulse responses may not be identically zero above order  $N$ . However, the finite sum of (2.3) implies that higher order terms contribute negligibly to the output.

The  $n$ th order nonlinear transfer function is defined to be the  $n$ -dimensional Fourier transform of  $h_n(\tau_1, \dots, \tau_n)$ . This results in the Fourier transform pair

$$H_n(f_1, \dots, f_n) = \int_{-\infty}^{\infty} h_n(\tau_1, \dots, \tau_n) \prod_{p=1}^n e^{-j2\pi f_p \tau_p} d\tau_p \quad (2.4)$$

$$h_n(\tau_1, \dots, \tau_n) = \int_{-\infty}^{\infty} H_n(f_1, \dots, f_n) \prod_{p=1}^n e^{j2\pi f_p \tau_p} df_p \quad (2.5)$$

Substitution of (2.5) into (2.3) yields the input-output relation

$$y(t) = \sum_{n=1}^N \int_{-\infty}^{\infty} H_n(f_1, \dots, f_n) \prod_{p=1}^n X(f_p) e^{j2\pi f_p t} df_p \quad (2.6)$$

where  $X(f)$  is the Fourier transform of the input  $x(t)$ . (2.3) and (2.6) suggest the block diagram representation shown in Figs. 1 and 2, respectively. The nonlinear system is completely characterized by either the nonlinear impulse responses or the nonlinear transfer functions. Once these are known, it is possible to determine the system response for arbitrary inputs.

The special case for which the input is a sum of  $M$  sinusoidal terms is of particular interest. Assume

$$x(t) = \sum_{m=1}^M |E_m| \cos(2\pi f_m t + \theta_m) \quad (2.7)$$

Define the complex voltage

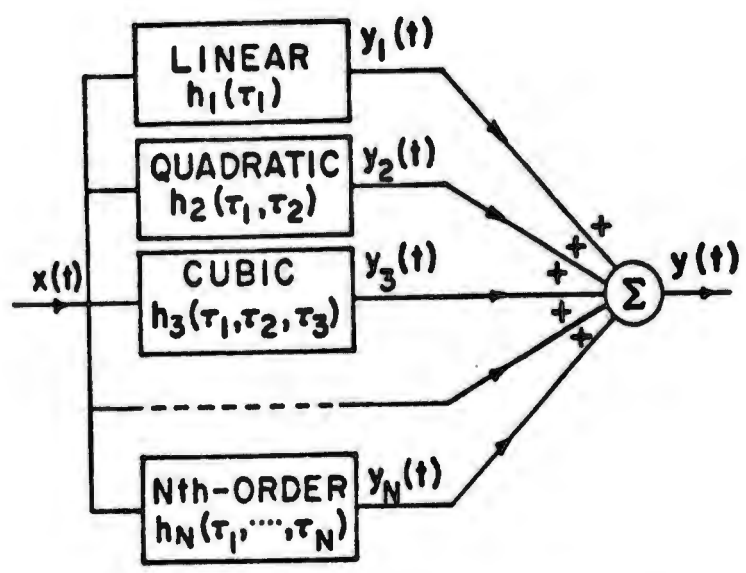


Figure 1. Characterization of a nonlinear system with memory in terms of its N impulse responses,  $h_n(\tau_1, \dots, \tau_n)$ ;  $n = 1, 2, \dots, N$ .

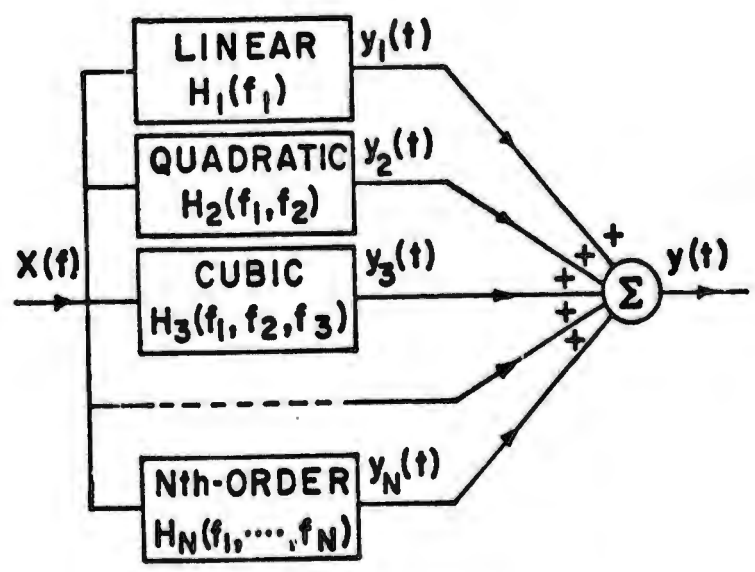


Figure 2. Characterization of a nonlinear system with memory in terms of its N transfer functions,  $H_n(f_1, \dots, f_n)$ ;  $n = 1, 2, \dots, N$ .

$$E_m = |E_m| e^{j\theta_m} \quad (2.8)$$

Let

$$f_{-m} = -f_m, E_0 = 0, \text{ and } E_{-m} = E_m^* \quad (2.9)$$

where the asterisk denotes complex conjugate. It follows that the input can be written as

$$x(t) = \frac{1}{2} \sum_{m=-M}^M E_m e^{j2\pi f_m t} \quad (2.10)$$

Substitution of (2.10) into (2.3) and use of (2.4) results in the response

$$\begin{aligned} y(t) = & \frac{1}{2} \sum_{m=-M}^M E_m H_1(f_m) e^{j2\pi f_m t} \\ & + \frac{1}{2^2} \sum_{m_1=-M}^M \sum_{m_2=-M}^M E_{m_1} E_{m_2} H_2(f_{m_1}, f_{m_2}) e^{j2\pi(f_{m_1} + f_{m_2})t} \\ & + \dots \\ & + \frac{1}{2^N} \sum_{m_1=-M}^M \dots \sum_{m_N=-M}^M E_{m_1} \dots E_{m_N} H_N(f_{m_1}, \dots, f_{m_N}) e^{j2\pi(f_{m_1} + \dots + f_{m_N})t} \end{aligned} \quad (2.11)$$

As expected, when a sum of  $M$  tones is applied to a nonlinear system of highest significant order  $N$ , additional frequencies are generated consisting of all possible combinations of the tones taken from one up to  $N$  at a time. (2.11) clearly demonstrates that  $H_n(f_1, \dots, f_n)$  is the nonlinear transfer function associated with the sinusoidal output at frequency  $(f_1 + \dots + f_n)$ . It can be shown that no loss in generality results if the nonlinear transfer functions are assumed to be perfectly symmetrical in their arguments. Note that Equation (2.11) involves the transfer functions which are frequency domain quantities. Thus, the time domain solution for individual frequency components in the response is obtained directly from

the frequency domain transfer functions without the need for performing a fast Fourier transform. This results in increased accuracy as far as determination of the powers associated with individual frequency components of the response are concerned.

The analysis of the single port nonlinearly loaded network described in [6] is now extended to nonlinearly loaded K-port networks where the Kth port is assumed to be linear.

### 3. MULTIPLE INPUT VOLTERRA SERIES

The Volterra series is a generalization of the Taylor series expansion for representing a nonlinear system. Thus the Volterra series for multiple-input systems is obtained by direct analogy to the corresponding multi-variable Taylor series. A multiple input Volterra series for a K-port network is given by

$$y^{(k)}(t) = \sum_{n=1}^{\infty} y_n^{(k)}(t), \quad k=1,2,\dots,K \quad (3.1)$$

where  $y^{(k)}(t)$  is the output observed at port k and  $y_n^{(k)}(t)$  is the nth order portion of the response at port k. It is given by

$$y_n^{(k)}(t) = \sum_{s_1=1}^K \dots \sum_{s_n=1}^K \int h_n^{(k;s_1,s_2,\dots,s_n)}(\tau_1,\dots,\tau_n) \prod_{p=1}^n x^{(s_p)}(t-\tau_p) d\tau_p \quad (3.2)$$

where  $x^{(s_p)}(t)$  is the applied input at port  $s_p$ .  $h_n^{(k;s_1,\dots,s_n)}(\tau_1,\dots,\tau_n)$

then represents the nth order nonlinear impulse response relating the output at port k to the inputs applied to ports  $s_1, s_2 \dots$  and  $s_n$ .

The nth order nonlinear transfer function  $H_n^{(k;s_1,\dots,s_n)}(f_1,\dots,f_n)$

is related to the  $n$ th order nonlinear impulse response of the network by the Fourier transform pair

$$H_n^{(k; s_1, \dots, s_n)}(f_1, \dots, f_n) = \int_{-\infty}^{\infty} h_n^{(k; s_1, s_2, \dots, s_n)}(\tau_1, \tau_2, \dots, \tau_n) \prod_{p=1}^n \exp[-j2\pi f_p \tau_p] d\tau_p \quad (3.3)$$

and

$$h_n^{(k; s_1, s_2, \dots, s_n)}(\tau_1, \tau_2, \dots, \tau_n) = \int_{-\infty}^{\infty} H_n^{(k; s_1, s_2, \dots, s_n)}(f_1, f_2, \dots, f_n) \prod_{p=1}^n \exp[j2\pi f_p \tau_p] df_p \quad (3.4)$$

Substitution of (3.3) into (3.2) yields the input-output relationship for the  $n$ th order response of  $K$ -port network.

$$y_n^{(k)}(t) = \sum_{s_1=1}^K \dots \sum_{s_n=1}^K \int_{-\infty}^{\infty} H_n^{(k; s_1, \dots, s_n)}(f_1, \dots, f_n) \prod_{p=1}^n X^{(s_p)}(f_p) \exp[j2\pi f_p t] df_p \quad (3.5)$$

where  $X^{(s_p)}(f)$  is the Fourier transform of the input  $x^{(s_p)}(t)$ .

The special case for which the input is a sum of  $M$  sinusoidal terms is of particular interest. Assume

$$x^{(s_p)}(t) = \sum_{m=1}^M |I^{(s_p)}(f_m)| \cos(2\pi f_m t + \theta_m) \quad (3.6)$$

where the complex input current is defined as

$$I^{(s_p)}(f_m) = |I^{(s_p)}(f_m)| e^{j\theta_m} \quad (3.7)$$

It follows that the input at port  $s_p$  can be written as

$$x(t) = \frac{1}{2} \sum_{m=-M}^M I^{(s_p)}(f_m) e^{j2\pi f_m t} \quad (3.8)$$

Substitution of (3.8) into (3.2) and use of (3.3) results in the response

$$\begin{aligned}
 y_n^{(k)}(t) = & \frac{1}{2^n} \sum_{s_1=1}^K \dots \sum_{s_n=1}^K \sum_{m_1=-M}^M \dots \sum_{m_n=-M}^M \\
 & H_n^{(k; s_1, \dots, s_n)}(f_{m_1}, \dots, f_{m_n}) I^{(s_1)}(f_{m_1}) \dots I^{(s_n)}(f_{m_n}) \\
 & e^{j2\pi(f_{m_1} + \dots + f_{m_n})t} \quad (3.9)
 \end{aligned}$$

It is seen that a nonlinear K-port network is completely characterized provided all possible interactions between the independent port variables are accounted for. Equations (3.1) and (3.9) give the total response at any of the ports  $k=1, \dots, K$  of a Volterra K-port network excited by sources as expressed in (3.8).

It is interesting to note from (3.9) that when  $f_{m_1}$  and  $f_{m_j}$  are interchanged in the argument of the nth order nonlinear transfer function, the final result for response  $y_n^{(k)}(t)$  remains the same provided  $s_1$  and  $s_j$  are also interchanged. For example,  $H_3^{(1;1,2,1)}(f_1, f_2, f_3) I^{(1)}(f_1) I^{(2)}(f_2) I^{(1)}(f_3)$  can be replaced by  $H_3^{(1;2,1,1)}(f_2, f_3, f_1) I^{(2)}(f_2) I^{(1)}(f_3) I^{(1)}(f_1)$  without altering the final result. This is a very important point which often simplifies the computation at different harmonic responses.

#### 4. DETERMINATION OF THE NONLINEAR TRANSFER FUNCTION

Nonlinear transfer functions can be determined from the circuit diagram of a system. If the nonlinearities are assumed to be diodes then the nonlinearly loaded K-port system can be represented by Fig. 3. The system consists of independent current generators  $I^{(1)}, I^{(2)}, \dots, I^{(K)}$ , the admittance matrix  $[Y]$  of the linear K-port network, and nonlinear loads at each of the K-ports, which are modelled by the linear capacitances  $C^{(k)}$

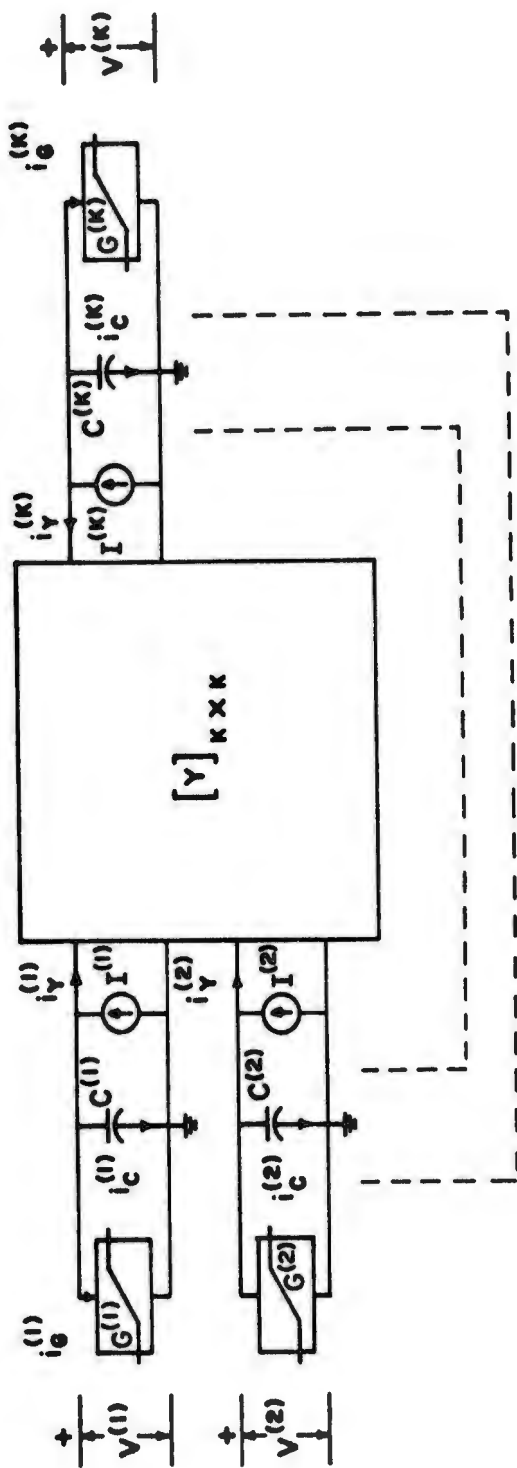


Fig. 3. Circuit with nonlinear conductors  $G^{(k)}$ .

and the nonlinear conductors  $G^{(k)}$ , for  $k=1,2,\dots,K$ . The current through the  $k$ th nonlinear conductor  $i_G^{(k)}$  can be represented as

$$i_G^{(k)} = f(v^{(k)}) \quad (4.1)$$

where  $f(\cdot)$  is a zero memory nonlinear function and  $v^{(k)}$  is the node to datum voltage at the  $k$ th port.

The first step in the nonlinear function approach is to expand  $f(v^{(k)})$  in a power series. For simplicity, assume that  $f(v^{(k)})$  is adequately characterized by the power series

$$i_G^{(k)} = a^{(k)}v^{(k)} + b^{(k)}\{v^{(k)}\}^3 \quad (4.2)$$

where  $a^{(k)}$  and  $b^{(k)}$  are constants pertaining to the nonlinear loads at the  $k$ th port. The  $i$ - $v$  relationships for the nonlinear conductors can be written collectively in matrix form as

$$\begin{bmatrix} i_G^{(1)} \\ i_G^{(2)} \\ \vdots \\ i_G^{(K)} \end{bmatrix}_{K \times 1} = \begin{bmatrix} a^{(1)} & & & \\ & a^{(2)} & & \\ & & \ddots & \\ & & & a^{(K)} \end{bmatrix}_{K \times K} \begin{bmatrix} v^{(1)} \\ v^{(2)} \\ \vdots \\ v^{(K)} \end{bmatrix}_{K \times 1} + \begin{bmatrix} b^{(1)} & & & \\ & b^{(2)} & & \\ & & \ddots & \\ & & & b^{(K)} \end{bmatrix}_{K \times K} \begin{bmatrix} \{v^{(1)}\}^3 \\ \{v^{(2)}\}^3 \\ \vdots \\ \{v^{(K)}\}^3 \end{bmatrix}_{K \times 1} \quad (4.3)$$

The column matrix  $[i_G^{(k)}]_{K \times 1}$  represents the currents through the  $K$  nonlinear conductors and  $[v^{(k)}]_{K \times 1}$  represents the voltages across them.

The diagonal matrices  $[a^{(k)}]_{K \times K}$  and  $[b^{(k)}]_{K \times K}$  contain the parameters of the nonlinear loads.

The second step is to write Kirchoff's current law equation at each node with node to datum voltage,  $v^{(k)}$ . Summation of the currents at the nodes results in the matrix equation

$$[I^{(k)}]_{K \times 1} = \{[i_G^{(k)}]\}_{K \times 1} + \{[i_Y^{(k)}]\}_{K \times 1} + \{[i_C^{(k)}]\}_{K \times 1} \quad (4.4)$$

where the currents with superscripts Y,C,G represent the currents in the linear K-port network, capacitance, and the nonlinear conductor, respectively. By expressing the currents in terms of  $v^{(k)}$ , the equation becomes

$$\begin{aligned} [I^{(k)}]_{K \times 1} = & [Y]_{K \times K} [v^{(k)}]_{K \times 1} + [a^{(k)}]_{K \times K} [v^{(k)}]_{K \times 1} \\ & + [b^{(k)}]_{K \times K} \{[v^{(k)}]^3\}_{K \times 1} \\ & + [C^{(k)}]_{K \times K} \left[ \frac{d v^{(k)}}{dt} \right]_{K \times 1} \end{aligned} \quad (4.5)$$

Rearranging terms by moving the nonlinear term to the right hand side of equation (4.5) yields

$$[C^{(k)}] \left[ \frac{d v^{(k)}}{dt} \right] + \{[Y] + [a^{(k)}]\} [v^{(k)}] = [I^{(k)}] - [b^{(k)}] \{[v^{(k)}]^3\} \quad (4.6)$$

Equation (4.6) can then be interpreted in terms of the network indicated in Fig. 4. The nonlinear conductors at each port have been replaced by linear conductors  $a^{(k)}$  in parallel with the voltage-controlled current sources  $b^{(k)} \{v^{(k)}\}^3$ .  $a^{(k)}$ , obtained from the linear term of the power series expansion of  $f(v^{(k)})$ , is the linear conductance that would be used in a linear incremental model of the network. The nonlinear portion

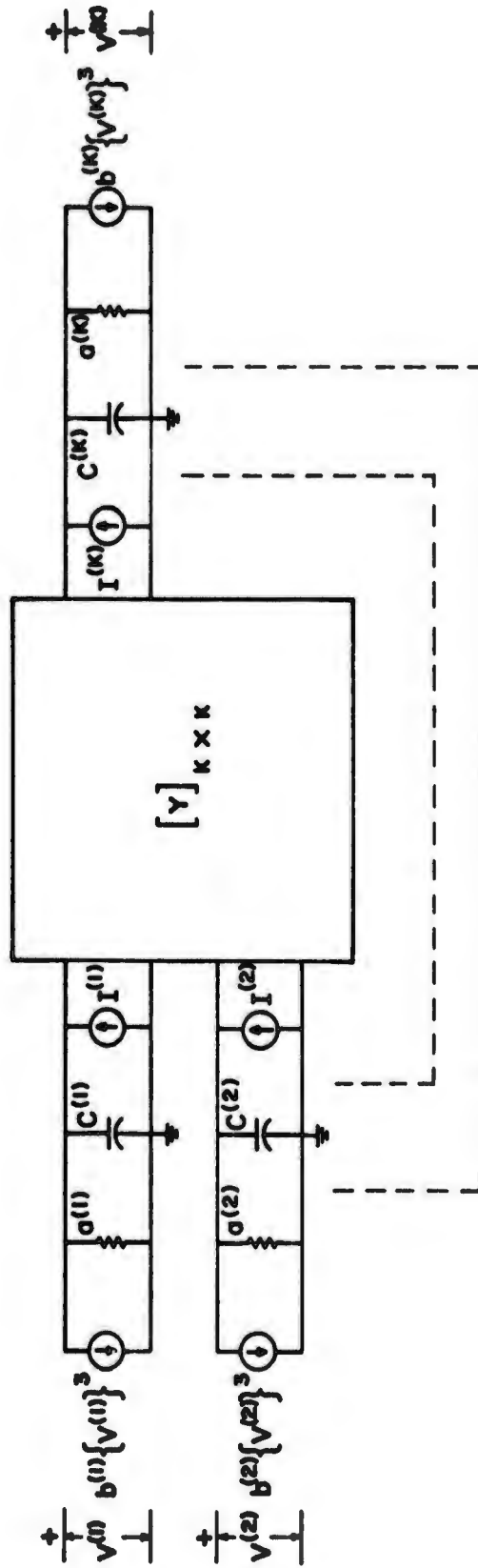


Fig. 4. Equivalent circuit of that shown in Fig. 3 for the special case  $i_G^{(k)} = a^{(k)}v^{(k)} + b^{(k)}\{v^{(k)}\}^3$ .

of  $G^{(k)}$  manifests itself as a dependent current source driving the linearized circuit. In terms of the operator  $D = \frac{d}{dt}$ , equation (4.6) can be written as

$$[A^{(k)}(D)] [V^{(k)}] = [I^{(k)}] - [b^{(k)}] [\{V^{(k)}\}^3] \quad (4.7)$$

where

$$[A^{(k)}(D)] = [Y(D)] + [a^{(k)}] + [C^{(k)}D] \quad (4.8)$$

It is now shown how to obtain the Volterra kernels.

Specialization to a two-port network: Consider the loaded nonlinear 2-port shown in Fig. 5. It is assumed that the nonlinearities at the two ports are adequately characterized by

$$\begin{bmatrix} i^{(1)} \\ i^{(2)} \end{bmatrix} = \begin{bmatrix} a^{(1)} & 0 \\ 0 & a^{(2)} \end{bmatrix} \begin{bmatrix} v^{(1)} \\ v^{(2)} \end{bmatrix} + \begin{bmatrix} b^{(1)} & 0 \\ 0 & b^{(2)} \end{bmatrix} \begin{bmatrix} \{v^{(1)}\}^3 \\ \{v^{(2)}\}^3 \end{bmatrix} \quad (4.9)$$

Let the independent current sources be the complex exponentials

$$\begin{bmatrix} I^{(1)}(t) \\ I^{(2)}(t) \end{bmatrix} = \begin{bmatrix} I^{(1)}(f) & \exp(j2\pi ft) \\ I^{(2)}(f) & \exp(j2\pi ft) \end{bmatrix} \quad (4.10)$$

Hence, the linear portion of the 2-port is characterized by

$$v_1^{(1)}(t) = [H_1^{(1;1)}(f) I^{(1)}(f) + H_1^{(1;2)}(f) I^{(2)}(f)] \exp(j2\pi ft) \quad (4.11.a)$$

and

$$v_1^{(2)}(t) = [H_1^{(2;1)}(f) I^{(1)}(f) + H_1^{(2;2)}(f) I^{(2)}(f)] \exp(j2\pi ft) \quad (4.11.b)$$

In (4.11) the subscript 1 indicates that all variables and parameters are of first order. The superscript (k); k=1,2, on the variables indicates the port with which they are associated. Finally the double superscript (j;m) (j,m=1,2) on the nonlinear transfer functions indicate that the corresponding dependent variable is at port j while the

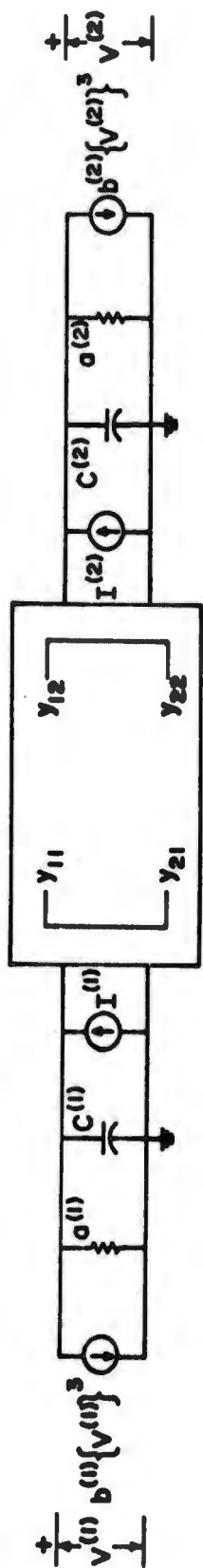


Fig. 5. Nonlinearly loaded 2-port.

corresponding independent variable is at port  $m$ . Observe that, as usual, four parameters are required to completely characterize the linear portion of the nonlinear 2-port.

The next step in the procedure is to obtain the nonlinear transfer functions for  $V^{(k)}$ . Using the Volterra approach,  $V^{(k)}(t)$  is written as in (3.1), where the  $n$ th order portion of the system response is given by (3.9).

To investigate the characterization of the second-order portion of the 2-port, assume sinusoidal excitations at frequencies  $f_1$  and  $f_2$ . In general, the second-order response at each port consists of a sum of sinusoids whose frequencies are the second harmonics and the sums and differences of the input frequencies. Hence the second order portion of the response can be expressed as

$$V_2^{(1)}(t) = \sum_{s_1=1}^2 \sum_{s_2=1}^2 \sum_{m_1=1}^2 \sum_{m_2=1}^2 I^{(s_1)}(f_{m_1}) I^{(s_2)}(f_{m_2}) H_2^{(1; s_1, s_2)}(f_{m_1}, f_{m_2}) \exp [j2\pi (f_{m_1} + f_{m_2})t] \quad (4.12)$$

and

$$V_2^{(2)}(t) = \sum_{s_1=1}^2 \sum_{s_2=1}^2 \sum_{m_1=1}^2 \sum_{m_2=1}^2 I^{(s_1)}(f_{m_1}) I^{(s_2)}(f_{m_2}) H_2^{(2; s_1, s_2)}(f_{m_1}, f_{m_2}) \exp [j2\pi (f_{m_1} + f_{m_2})t] \quad (4.13)$$

Let the response at the sum frequency  $(f_1 + f_2)$  be of interest. To completely characterize the second-order portion of the nonlinear 2-port, it is necessary to account for each of the possible mechanisms by which components  $(f_1 + f_2)$  may be generated in the port voltages. Accordingly,

$$\begin{aligned}
v_2^{(1)}(t) = & [H_2^{(1;1,1)}(f_1, f_2) I^{(1)}(f_1) I^{(1)}(f_2) + H_2^{(1;1,1)}(f_2, f_1) I^{(1)}(f_2) I^{(1)}(f_1) \\
& + H_2^{(1;1,2)}(f_1, f_2) I^{(1)}(f_1) I^{(2)}(f_2) + H_2^{(1;1,2)}(f_2, f_1) I^{(1)}(f_2) I^{(2)}(f_1) \\
& + H_2^{(1;2,1)}(f_1, f_2) I^{(2)}(f_1) I^{(1)}(f_2) + H_2^{(1;2,1)}(f_2, f_1) I^{(2)}(f_2) I^{(1)}(f_1) \\
& + H_2^{(1;2,2)}(f_1, f_2) I^{(2)}(f_1) I^{(2)}(f_2) + H_2^{(1;2,2)}(f_2, f_1) I^{(2)}(f_2) I^{(2)}(f_1)] \\
& \times \exp [j2\pi (f_1 + f_2)t] \tag{4.14}
\end{aligned}$$

Similarly,  $v_2^{(2)}(t)$  for this particular  $(f_1 + f_2)$  component can be obtained from (4.13). In (4.12) and (4.13) the subscripts and superscripts have the same interpretation as in (4.11). However, now the triple superscript  $(l; m, j)$  ( $l, m, j=1, 2$ ) on the 2-port parameters  $H_2^{(l; m, j)}(f_a, f_b)$  indicates that the corresponding dependent variable is at port  $l$  while the corresponding independent variable at  $f_a$  is at port  $m$  and the corresponding independent variable at  $f_b$  is at port  $j$ . For example,  $H_2^{(1; 2, 1)}(f_1, f_2)$  is the transfer function relating that portion of the second-order voltage response at port 1 and frequency  $(f_1 + f_2)$  due to the mix of the linear portion of the current at port 2 and frequency  $f_1$  with the linear portion of the current at port 1 and frequency  $f_2$ . Note that eight second-order parameters are needed in addition to the four linear parameters in order to completely characterize the second-order behavior of the 2-port. In general,  $2^{n+1}$  nth order parameters are needed in the characterization of the nth order portion of a nonlinear 2-port. For a nonlinear K-port network  $K^{n+1}$  nth order parameters are needed to completely specify the network.

Hence, if the current excitation at port  $s_p$  is assumed of the form

$$I^{(s_p)}(t) = I^{(s_p)}(f) \exp(j2\pi ft) \quad (4.15)$$

then the voltage at the  $k$ th port can be written as

$$\begin{aligned} v^{(k)}(t) &= v_1^{(k)}(t) + v_2^{(k)}(t) + v_3^{(k)}(t) + \dots \\ &= \sum_{s_1=1}^2 H_1^{(k; s_1)}(f) I^{(s_1)}(f) \exp(j2\pi ft) \\ &+ \sum_{s_1=1}^2 \sum_{s_2=1}^2 H_2^{(k; s_1, s_2)}(f, f) I^{(s_1)}(f) I^{(s_2)}(f) \exp(j4\pi ft) \\ &+ \sum_{s_1=1}^2 \sum_{s_2=1}^2 \sum_{s_3=1}^2 H_3^{(k; s_1, s_2, s_3)}(f, f, f) I^{(s_1)}(f) I^{(s_2)}(f) I^{(s_3)}(f) \\ &\quad \exp(j6\pi ft) \\ &+ \dots \end{aligned} \quad (4.16)$$

Substitution of  $v^{(k)}(t)$  and  $I^{(k)}(t)$  into the network equation (4.7) yields

$$\begin{aligned} [A^{(k)}(D)]_{2 \times 2} [V^{(k)}(t)]_{2 \times 1} &= \begin{bmatrix} I^{(1)}(f) \exp(j2\pi ft) \\ I^{(2)}(f) \exp(j2\pi ft) \end{bmatrix}_{2 \times 1} \\ &- [b^{(k)}]_{2 \times 2} [I^{(k)}]_{2 \times 1} \end{aligned} \quad (4.16)$$

$$\begin{aligned} [A^{(k)}(D)]_{2 \times 2} &\left[ \sum_{s_1=1}^2 H_1^{(k; s_1)}(f) I^{(s_1)}(f) \exp(j2\pi ft) + \sum_{s_1=1}^2 \sum_{s_2=1}^2 H_2^{(k; s_1, s_2)}(f, f) I^{(s_1)}(f) \right. \\ &\times I^{(s_2)}(f) \exp(j4\pi ft) + \sum_{s_1=1}^2 \sum_{s_2=1}^2 \sum_{s_3=1}^2 H_3^{(k; s_1, s_2, s_3)}(f, f, f) I^{(s_1)}(f) I^{(s_2)}(f) I^{(s_3)}(f) \\ &\quad \left. \exp(j6\pi ft) + \dots \right]_{2 \times 1} \\ &= [I^{(k)} \exp(j2\pi ft)]_{2 \times 1} - [b^{(k)}]_{2 \times 2} \left[ \sum_{s_1=1}^2 \sum_{s_2=1}^2 \sum_{s_3=1}^2 H_1^{(k; s_1)}(f) I^{(s_1)}(f) \right. \\ &\quad \left. H_1^{(k; s_2)}(f) I^{(s_2)}(f) H_1^{(k; s_3)}(f) I^{(s_3)}(f) \exp(j6\pi ft) + \dots \right]_{2 \times 1} \end{aligned} \quad (4.18)$$

Utilizing the linear independence property of the exponentials it is possible to equate terms on each side of the equation involving  $\exp(j2\pi ft)$ . It follows that

$$[A^{(k)}(D)] \begin{bmatrix} H^{(1;1)}(f) & H^{(1;2)}(f) \\ H^{(2;1)}(f) & H^{(2;2)}(f) \end{bmatrix} \begin{bmatrix} I^{(1)} \exp(j2\pi ft) \\ I^{(2)} \exp(j2\pi ft) \end{bmatrix} = \begin{bmatrix} I^{(1)} \exp(j2\pi ft) \\ I^{(2)} \exp(j2\pi ft) \end{bmatrix} \quad (4.19)$$

Substitution for  $[A^{(k)}(D)]$  in the above equation and carrying out the differentiation yields

$$\{[j2\pi f C^{(k)}] + [a^{(k)}] + [Y(f)]\} \begin{bmatrix} H_1^{(1;1)}(f) & H_1^{(1;2)}(f) \\ H_1^{(2;1)}(f) & H_1^{(2;2)}(f) \end{bmatrix} = [U] \quad (4.20)$$

where  $[U]$  is the unit matrix. Therefore,

$$\begin{bmatrix} H_1^{(1;1)}(f) & H_1^{(1;2)}(f) \\ H_1^{(2;1)}(f) & H_1^{(2;2)}(f) \end{bmatrix} = \begin{bmatrix} j2\pi f C^{(1)} + a^{(1)} + y_{11}(f) & y_{12}(f) \\ y_{21}(f) & j2\pi f C^{(2)} + a^{(2)} + y_{22}(f) \end{bmatrix}^{-1} \quad (4.21)$$

It is seen that the transfer functions  $H_1^{(j;k)}(f)$  have the same interpretation as the Z-parameters of the two port network.  $H_1^{(1;1)}(f)$  and  $H_1^{(2;2)}(f)$  are the input impedances and  $H_1^{(1;2)}(f)$  and  $H_1^{(2;1)}(f)$  are characterized by the transfer impedances of the network. The characteristics at any other frequency can be obtained by computing the impedances for that frequency.

Equating terms on each side of (4.18) involving  $\exp(j4\pi ft)$  yields

$$[A^{(k)}(n)]_{2 \times 2} \begin{bmatrix} \sum_{s_1=1}^2 \sum_{s_2=1}^2 H_2^{(1; s_1, s_2)}(f, f) I^{(s_1)}(f) I^{(s_2)}(f) \\ \sum_{s_1=1}^2 \sum_{s_2=1}^2 H_2^{(2; s_1, s_2)}(f, f) I^{(s_1)}(f) I^{(s_2)}(f) \end{bmatrix} = [0] \quad (4.22)$$

This implies

$$\sum_{s_1=1}^2 \sum_{s_2=1}^2 H_2^{(k; s_1, s_2)}(f, f) I^{(s_1)}(f) I^{(s_2)}(f) = 0 \quad \text{for } k=1,2 \quad (4.23)$$

Since (4.23) holds for all possible values of  $I^{(s_1)}(f)$  and  $I^{(s_2)}(f)$ ,

it follows that

$$H_2^{(k; s_1, s_2)}(f, f) = 0 \quad \text{for } k, s_1 \text{ and } s_2 = 1,2 \quad (4.24)$$

Similarly, equating terms on each side of (4.18) involving  $\exp(j6\pi ft)$  yields

$$[A^{(k)}(3f)] \begin{bmatrix} \sum_{s_1=1}^2 \sum_{s_2=1}^2 \sum_{s_3=1}^2 H_3^{(1; s_1, s_2, s_3)}(f, f, f) I^{(s_1)}(f) I^{(s_2)}(f) I^{(s_3)}(f) \\ \sum_{s_1=1}^2 \sum_{s_2=1}^2 \sum_{s_3=1}^2 H_3^{(2; s_1, s_2, s_3)}(f, f, f) I^{(s_1)}(f) I^{(s_2)}(f) I^{(s_3)}(f) \end{bmatrix} \\ = - \begin{bmatrix} b^{(1)} & 0 \\ 0 & b^{(2)} \end{bmatrix} \begin{bmatrix} \sum_{s_1=1}^2 \sum_{s_2=1}^2 \sum_{s_3=1}^2 H_1^{(1; s_1)}(f) H_1^{(1; s_2)}(f) H_1^{(1; s_3)}(f) I^{(s_1)}(f) I^{(s_2)}(f) I^{(s_3)}(f) \\ \sum_{s_1=1}^2 \sum_{s_2=1}^2 \sum_{s_3=1}^2 H_1^{(2; s_1)}(f) H_1^{(2; s_2)}(f) H_1^{(2; s_3)}(f) I^{(s_1)}(f) I^{(s_2)}(f) I^{(s_3)}(f) \end{bmatrix} \quad (4.25)$$

After some algebraic manipulations the above equation can be reduced to the form

$$\sum_{s_1=1}^2 \sum_{s_2=1}^2 \sum_{s_3=1}^2 [A^{(k)}(3f)] \begin{bmatrix} H_3^{(1;s_1,s_2,s_3)}(f,f,f) \\ H_3^{(2;s_1,s_2,s_3)}(f,f,f) \end{bmatrix} + \begin{bmatrix} b^{(1)} & 0 \\ 0 & b^{(2)} \end{bmatrix} \begin{bmatrix} H_1^{(1;s_1)}(f)H_1^{(1;s_2)}(f)H_1^{(1;s_3)}(f) \\ H_1^{(2;s_1)}(f)H_1^{(2;s_2)}(f)H_1^{(2;s_3)}(f) \end{bmatrix}$$

$$I^{(s_1)}(f) I^{(s_2)}(f) I^{(s_3)}(f) = [0] \quad (4.26)$$

Equation (4.26) holds for all possible values of  $I^{(s_1)}(f)$ ,  $I^{(s_2)}(f)$  and  $I^{(s_3)}(f)$ .

Thus, the 3rd order nonlinear transfer functions are given by

$$\begin{aligned} H_3^{(1;s_1,s_2,s_3)}(f,f,f) &= - \begin{bmatrix} j6\pi fC^{(1)} + a^{(1)} + y_{11}(3f) & y_{12}(3f) \\ y_{21}(3f) & j6\pi fC^{(2)} + a^{(2)} + y_{22}(3f) \end{bmatrix}^{-1} \\ H_3^{(2;s_1,s_2,s_3)}(f,f,f) &= \begin{bmatrix} b^{(1)}H_1^{(1;s_1)}(f)H_1^{(1;s_2)}(f)H_1^{(1;s_3)}(f) \\ b^{(2)}H_1^{(2;s_1)}(f)H_1^{(2;s_2)}(f)H_1^{(2;s_3)}(f) \end{bmatrix} \end{aligned} \quad (4.27)$$

Since all arguments in  $H_2^{(k;s_1,s_2)}(f,f)$  and  $H_3^{(k;s_1,s_2,s_3)}(f,f,f)$  are evaluated at the same frequency  $f$ , the second and the third order transfer functions obtained in the above manner are useful for relating the input only to its second and the third harmonics, respectively. To obtain a more general expression for  $H_3^{(k;s_1,s_2,s_3)}(f_1,f_2,f_3)$  the inputs are chosen as

$$\begin{aligned} I^{(k)}(t) &= I^{(k)}(f_1) \exp(j2\pi f_1 t) + I^{(k)}(f_2) \exp(j2\pi f_2 t) \\ &+ I^{(k)}(f_3) \exp(j2\pi f_3 t) \\ &= \sum_{m=1}^3 I^{(k)}(f_m) \exp(j2\pi f_m t) \end{aligned} \quad (4.28)$$

where  $I^{(k)}(f_m)$  represent the complex amplitude of the input frequency  $f_m$

at port  $k$ .

By assuming that  $f_1, f_2,$  and  $f_3$  are incommensurable positive distinct frequencies, the  $p$ th order term in (3.9) becomes

$$v_p^{(k)}(t) = \sum_{s_1=1}^2 \dots \sum_{s_p=1}^2 \sum_{m_1=1}^3 \dots \sum_{m_p=1}^3 H_p^{(k; s_1, s_2, \dots, s_p)}(f_{m_1}, f_{m_2}, \dots, f_{m_p}) \exp \{j2\pi t(f_{m_1} + f_{m_2} + \dots + f_{m_p})\} \quad (4.29)$$

Substitution for  $I^{(k)}(t)$  and  $v^{(k)}(t)$  in (4.7) leads to

$$\begin{aligned} [A^{(k)}(D)]_{2 \times 2} & \left[ \sum_{m=1}^3 \sum_{s_1=1}^2 H_1^{(k; s_1)}(f_m) I^{(s_1)}(f_m) \exp(j2\pi f_m t) + \sum_{s_1=1}^2 \sum_{s_2=1}^2 \sum_{m_1=1}^3 \sum_{m_2=1}^3 \right. \\ & H_2^{(k; s_1, s_2)}(f_{m_1}, f_{m_2}) I^{(s_1)}(f_{m_1}) I^{(s_2)}(f_{m_2}) \exp \{j2\pi(f_{m_1} + f_{m_2})t\} \\ & + \sum_{m_1=1}^3 \sum_{m_2=1}^3 \sum_{m_3=1}^3 \sum_{s_1=1}^2 \sum_{s_2=1}^2 \sum_{s_3=1}^2 H_3^{(k; s_1, s_2, s_3)}(f_{m_1}, f_{m_2}, f_{m_3}) I^{(s_1)}(f_{m_1}) I^{(s_2)}(f_{m_2}) \\ & \left. I^{(s_3)}(f_{m_3}) \exp \{j2\pi(f_{m_1} + f_{m_2} + f_{m_3})t\} + \dots \right]_{2 \times 1} \\ & = \left[ \sum_{m=1}^3 I^{(k)}(f_m) \exp(j2\pi f_m t) \right]_{2 \times 1} \\ & - [b^{(k)}]_{2 \times 2} \left[ \sum_{m_1=1}^3 \sum_{m_2=1}^3 \sum_{m_3=1}^3 \sum_{s_1=1}^2 \sum_{s_2=1}^2 \sum_{s_3=1}^2 H_1^{(k; s_1)}(f_{m_1}) I^{(s_1)}(f_{m_1}) \right. \\ & \times H_1^{(k; s_2)}(f_{m_2}) I^{(s_2)}(f_{m_2}) H_1^{(k; s_3)}(f_{m_3}) I^{(s_3)}(f_{m_3}) \exp \{j2\pi(f_{m_1} + f_{m_2} + f_{m_3})t\} \\ & \left. + \dots \right]_{2 \times 1} \quad (4.30) \end{aligned}$$

The same arguments which were presented in the derivation of (4.24) can

also be applied to terms involving  $\exp \{j2\pi(f_{m_1} + f_{m_2})t\}$  on both sides of equation (4.30) to show that

$$H_2^{(k; s_1, s_2)}(f_1, f_2) = 0 \quad \text{for } k, s_1 \text{ and } s_2 = 1, 2 \quad (4.31)$$

By equating terms involving  $\exp j2\pi(f_1 + f_2 + f_3)t$  on both sides of (4.29),

$$\begin{aligned} & [A^{(k)}(D)]_{2 \times 2} \left[ \sum_{m_1=1}^3 \sum_{m_2=1}^3 \sum_{m_3=1}^3 \sum_{s_1=1}^2 \sum_{s_2=1}^2 \sum_{s_3=1}^2 H_3^{(k; s_1, s_2, s_3)}(f_{m_1}, f_{m_2}, f_{m_3}) \right. \\ & \quad \left. I^{(s_1)}(f_{m_1}) I^{(s_2)}(f_{m_2}) I^{(s_3)}(f_{m_3}) \right]_{2 \times 1} \\ & = - [b^{(k)}]_{2 \times 2} \left[ \sum_{m_1=1}^3 \sum_{m_2=1}^3 \sum_{m_3=1}^3 \sum_{s_1=1}^2 \sum_{s_2=1}^2 \sum_{s_3=1}^2 H_1^{(k; s_1)}(f_{m_1}) I^{(s_1)}(f_{m_1}) \right. \\ & \quad \left. H_1^{(k; s_2)}(f_{m_2}) I^{(s_2)}(f_{m_2}) H_1^{(k; s_3)}(f_{m_3}) I^{(s_3)}(f_{m_3}) \right]_{2 \times 1} \quad (4.32) \end{aligned}$$

Equation (4.32) can be rewritten in the following form:

$$\begin{aligned} & \sum_{m_1=1}^3 \sum_{m_2=1}^3 \sum_{m_3=1}^3 \sum_{s_1=1}^2 \sum_{s_2=1}^2 \sum_{s_3=1}^2 \{ [A^{(k)}(D)]_{2 \times 2} [H_3^{(k; s_1, s_2, s_3)}(f_{m_1}, f_{m_2}, f_{m_3})]_{2 \times 1} \\ & \quad + [b^{(k)}]_{2 \times 2} [H_1^{(k; s_1)}(f_{m_1}) H_1^{(k; s_2)}(f_{m_2}) H_1^{(k; s_3)}(f_{m_3})]_{2 \times 1} \} I^{(s_1)}(f_{m_1}) I^{(s_2)}(f_{m_2}) I^{(s_3)}(f_{m_3}) \\ & = [0] \quad (4.33) \end{aligned}$$

Since (4.33) is valid for all possible values of  $I^{(s_1)}(f_{m_1})$ ,  $I^{(s_2)}(f_{m_2})$  and  $I^{(s_3)}(f_{m_3})$ , it follows that the third order transfer function vector can be written in the following form

$$\begin{aligned}
 & \begin{bmatrix} H_3^{(1; s_1, s_2, s_3)}(f_1, f_2, f_3) \\ H_3^{(2; s_1, s_2, s_3)}(f_1, f_2, f_3) \end{bmatrix} = - \begin{bmatrix} j2\pi(f_1+f_2+f_3)C^{(1)} + a^{(1)} + y_{11}(f_1+f_2+f_3) & y_{12}(f_1+f_2+f_3) \\ y_{21}(f_1+f_2+f_3) & j2\pi(f_1+f_2+f_3)C^{(2)} + a^{(2)} + y_{22}(f_1+f_2+f_3) \end{bmatrix}^{-1} \\
 & \quad \times \begin{bmatrix} b^{(1)} & H_1^{(1; s_1)}(f_2) & H_1^{(1; s_2)}(f_2) & H_1^{(1; s_3)}(f_3) \\ b^{(2)} & H_1^{(2; s_1)}(f_1) & H_1^{(2; s_2)}(f_2) & H_1^{(2; s_3)}(f_3) \end{bmatrix} \quad (4.34)
 \end{aligned}$$

Thus  $H_3^{(k; s_1, s_2, s_3)}(f_1, f_2, f_3)$  depends only on  $[b^{(k)}]$  and the linear impedances of the linearized network.

In general, it can be shown that the characterization of the linearized multi-port network is extremely important when determining any of the nonlinear transfer functions. It can be shown that the assumption of positive distinct incommensurable frequencies is not necessary and that (4.2) is valid for all possible frequencies, both positive and negative.

The procedure for determining the higher-order kernels  $H_p^{(k; s_1, s_2, \dots, s_p)}(f_1, f_2, \dots, f_p)$  proceeds in a similar manner.

## 5. APPLICATION OF VOLTERRA SERIES TO A NONLINEARLY LOADED ANTENNA STRUCTURE

The Volterra series technique is now applied to the analysis of two center loaded thin dipole antennas illuminated by an E-field parallel to the dipole from the broadside direction with intensity

$$E^1 = E_0 \exp(j2\pi ft) \quad (5.1)$$

The nonlinear diode consists of two similar diodes connected as shown in Fig. 6. A Norton's equivalent network looking toward the scatter at the load ports aa' and bb' is determined by the method of moments [9-10] as

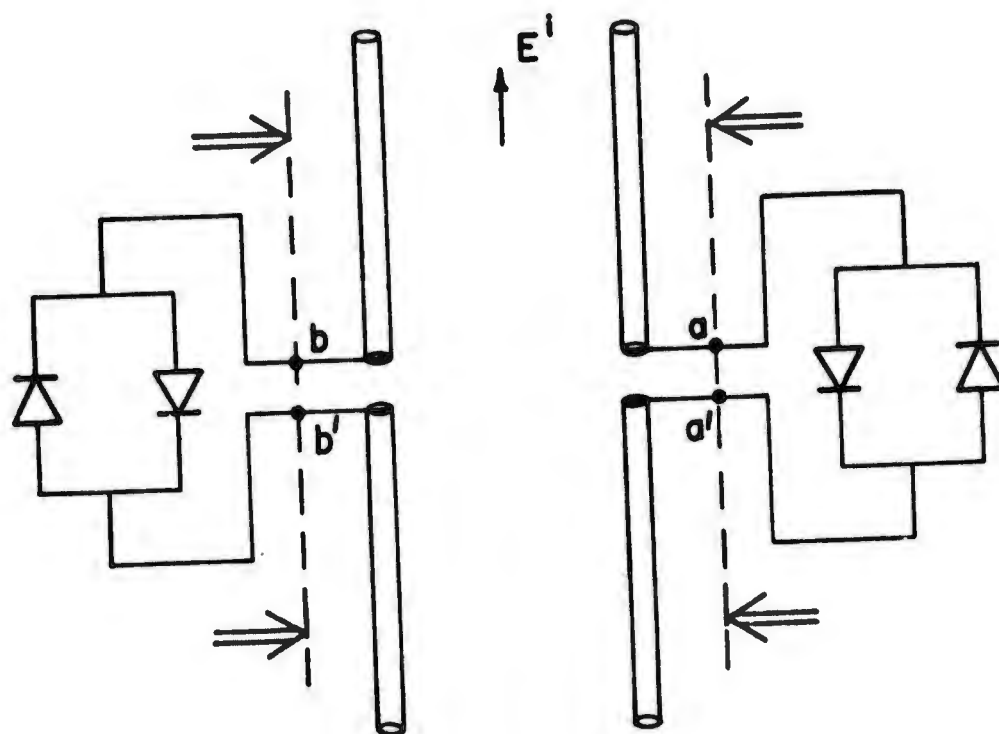


Fig. 6. Nonlinearly loaded antenna structure.

shown in Figure 7. If the structure is situated over an imperfect ground plane instead of free space, then the effects of the imperfect ground plane can be taken into account either exactly by the Sommerfeld formulation [11-13] or in an approximate manner by the Reflection Coefficient Method [13-16] for determining the Norton's equivalent. The method of moments, therefore, reduces the field problem into a K-port network problem.  $I^{(1)}$  and  $I^{(2)}$  are the short circuit currents due to the incident field  $E^i$ .

The i-v characteristic of the nonlinear devices is an odd symmetric function due to the arrangement of the diodes and can be represented as

$$i = d_1 v + d_3 v^3 + d_5 v^5 + \dots + d_n v^n \quad (5.2)$$

for odd integer values of n. For simplicity, the i-v characteristic of the nonlinear load is considered to be adequately approximated by

$$i = a \{V\} + b\{V\}^3 \quad (5.3)$$

The excitation is chosen of the form

$$I^{(k)} = I^{(k)}(f) \exp(j2\pi ft) \quad (5.4)$$

Responses above third-order are assumed to be negligible. Hence by recognizing that  $H_2^{(k;s_1,s_2)} = 0$ , the voltage  $V^{(k)}$  at port k is given by

$$\begin{aligned} V^{(k)}(t) = & \sum_{s_1=1}^2 H_1^{(k;s_1)}(f) I^{(s_1)}(f) \exp(j2\pi ft) \\ & + \sum_{s_1=1}^2 \sum_{s_2=1}^2 \sum_{s_3=1}^2 H_3^{(k;s_1,s_2,s_3)}(f,f,f) I^{(s_1)}(f) I^{(s_2)}(f) I^{(s_3)}(f) \\ & \exp\{j2\pi(3f)t\} \end{aligned} \quad (5.5)$$

From (5.3) and (5.5) the current at different harmonic frequencies

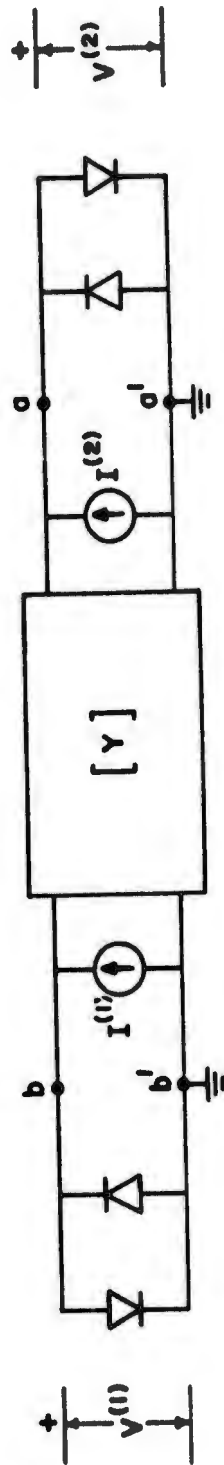


Fig. 7. Equivalent circuit of the nonlinearly loaded structure.

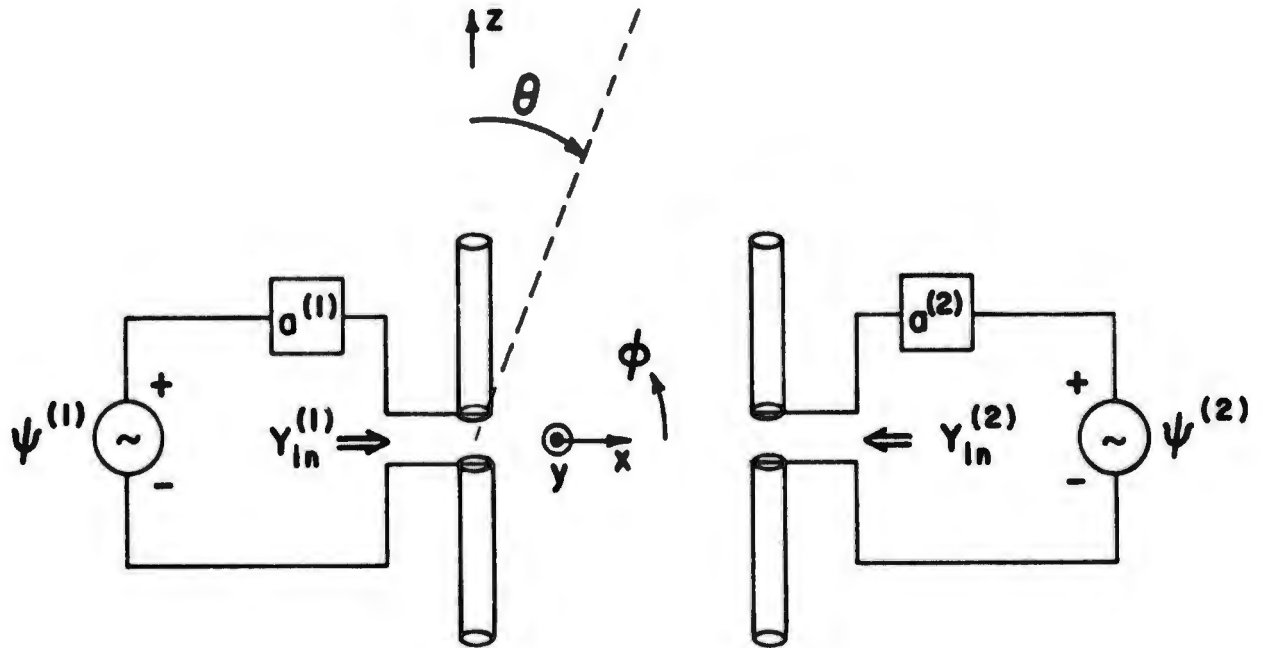
through the nonlinear load can be obtained. A case of interest is the scattered fields at the different harmonic frequencies which may cause interference with nearby receivers. The scattered fields are obtained by exciting the antenna structure with voltage sources at different harmonic frequencies. The magnitude of the voltage source is obtained from the voltage that exists across the nonlinear load at each port. The voltage-sources exciting the antenna at each port is related to  $v^{(k)}(t)$  by a multiplicative constant which depends on the linear conductance of the nonlinear load and the input admittance of the antenna structure seen from that port, as illustrated in Figure 8.

## 6. RESULTS

The system selected for analysis consists of two center loaded dipoles of lengths  $\frac{1}{3}m$  and radius 0.007m separated by 0.25m simultaneously excited by an impressed field of 1mV/m at 300 MHz(f). The nonlinear load consists of two MS-5231 diodes connected as shown in Figure 6. The coefficients 'a' and 'b' for the nonlinear loads are chosen as  $a = 0.0045 \text{ A/V}$  and  $b = 0.41 \text{ A/V}^3$ . The scattered field from the antenna structure contains many components at frequencies such as f, 3f, 5f, and so on. To obtain the field strength at different harmonic frequencies the voltages across the nonlinear loads are determined at those frequencies of interest. The antenna structure is then excited by these voltages at different harmonic frequencies to give the scattered field.

The voltages across the nonlinear loads are obtained from (5.5) as

$$\begin{aligned} v^{(1)}(t) &= v^{(2)}(t) \\ &= 0.145024 \underline{/75.67} \exp(j2\pi ft) \\ &+ 0.080874 \exp(j6\pi ft) + \dots \end{aligned}$$



$$\psi^{(k)} = .080875 [1 + Y_{in}^{(k)} + a^{(k)}] \quad \text{for } k = 1, 2$$

Fig. 8. Equivalent radiation problem for finding the scattered field at the harmonic frequency.

Hence the origin of the third harmonic frequency in the scattered field is the  $\exp(j6\pi ft)$  source that exists at the input port of the antenna structure. The scattered fields at the third harmonic frequency can be computed from the equivalent circuit of Figure 8. In this case two antenna elements are excited by voltages  $\psi^{(k)}$ , given by  $0.080874 [1 + Y_{in}^{(k)}(3f)/a^{(k)}]$  for  $k=1,2$ . The field pattern for the antenna array is computed for this excitation and is presented in Figure 9 for  $\theta = 90^\circ$ . The field pattern for this example produces nulls in the direction  $\phi = 48^\circ, 132^\circ, 228^\circ, \text{ and } 312^\circ$ . The directions which  $\phi$  and  $\theta$  are measured for Figure 9 are indicated in Figure 8. When one of the antennas is not nonlinearly loaded the problem of finding the scattered field at the third harmonic frequency is equivalent to computing the field pattern of two elements when only one element is excited. The pattern is given in Fig. 10. For this case there is no null in the pattern. The field strength for  $\phi$  greater than  $180^\circ$  is equal to the field strength at  $(360^\circ - \phi)$ , and is given by Figures 9 and 10.

This implies that on occasions additional nonlinear loads may be added to a system which is inherently nonlinear to produce a null in the fields at harmonic frequencies of interest in the direction of the receiver. For all these cases, it is interesting to note that the field pattern for the fundamental frequency remains totally unchanged.

If a nonlinear load already exists on antenna 1 and it is required to find another load on antenna 2 that will produce a null of the scattered field at the third harmonic in the direction  $\phi = \phi_1$ , then the problem can be approached as follows. First, the excitation voltages  $\psi^{(k)}$  at the third harmonic frequency to be applied to the antenna array are determined so

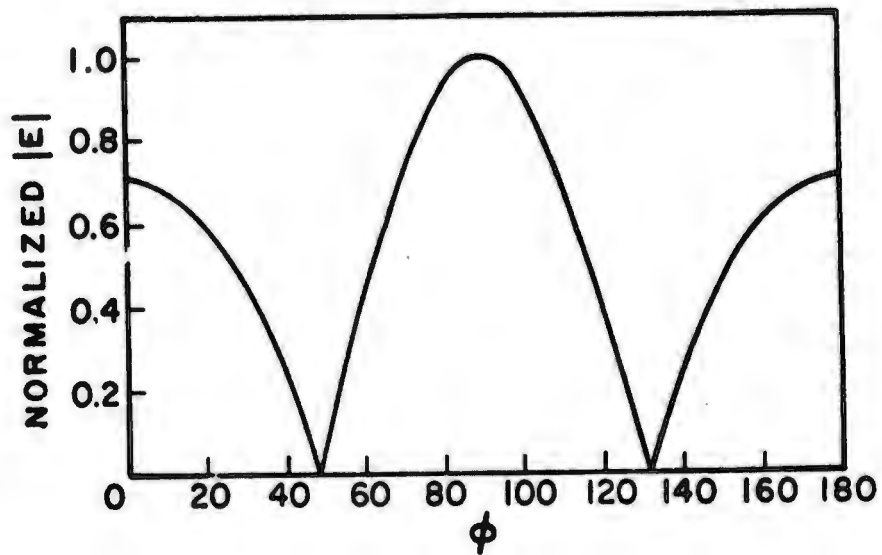


Fig. 9. Scattered field strength for the third harmonic frequency when two elements are nonlinearly loaded.

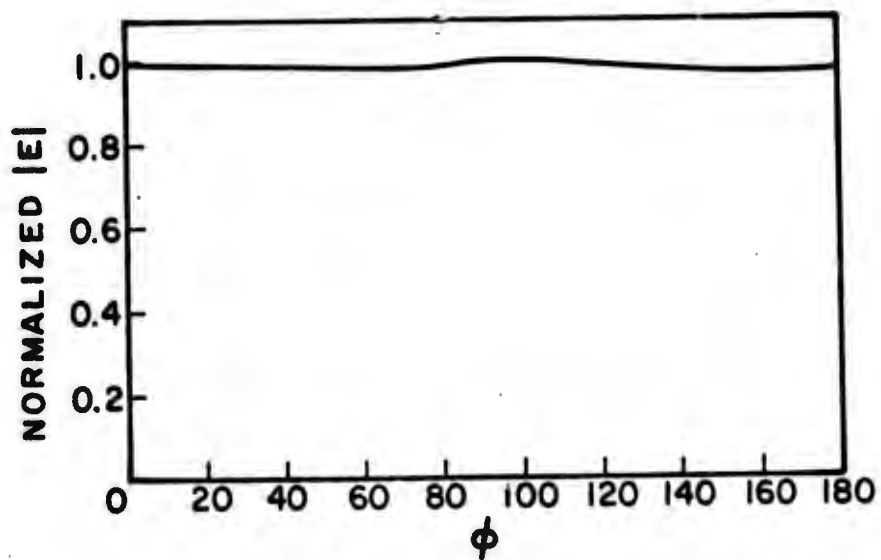


Fig. 10. Scattered field strength at the third harmonic frequency when one element is nonlinearly loaded.

that the field pattern of the structure has a null in the direction  $\phi = \phi_1$ . Next, the coefficients  $a^{(2)}$  and  $b^{(2)}$  of the nonlinear load are chosen by an optimization procedure to obtain the desired voltages  $\psi^{(k)}$  in the response  $V^{(1)}(t)$  and  $V^{(2)}(t)$ . This does not imply that there would be a cancellation at other odd harmonics. Since it is assumed that the higher-order terms are much smaller, they can be neglected.

#### 7. IMPLICATIONS OF THE RESULT

Rivets on a parabolic reflector sometimes cause nonlinear scattering [17]. The rivets used on a parabolic reflector with aging form a metal insulator metal junction whose  $i-v$  characteristics are very similar to two diodes connected back to back. Hence, according to the present analysis they could be treated as nonlinear loads. Now in order to find the total response at the required harmonic frequency Higa [17] just multiplies the response from one rivet by the total number of rivets on the reflector. But this is really not justified. The position of the rivets can be utilized to cause destructive interference at the focus rather than constructive interference. So, if two layers of rivets are placed in such a way that the path difference is of the order of  $\lambda/2$  for the third harmonic, as shown in Figure 11, for a certain frequency than the total response from the two layers as shown would cause destructive interference at the focus where the receiver might be placed. But in actual practice the rivets might not age uniformly and hence their  $i-v$  characteristics might not be the same, or because of slightly different sizes and shapes there still might be a small residual field at the undesired harmonic frequency.

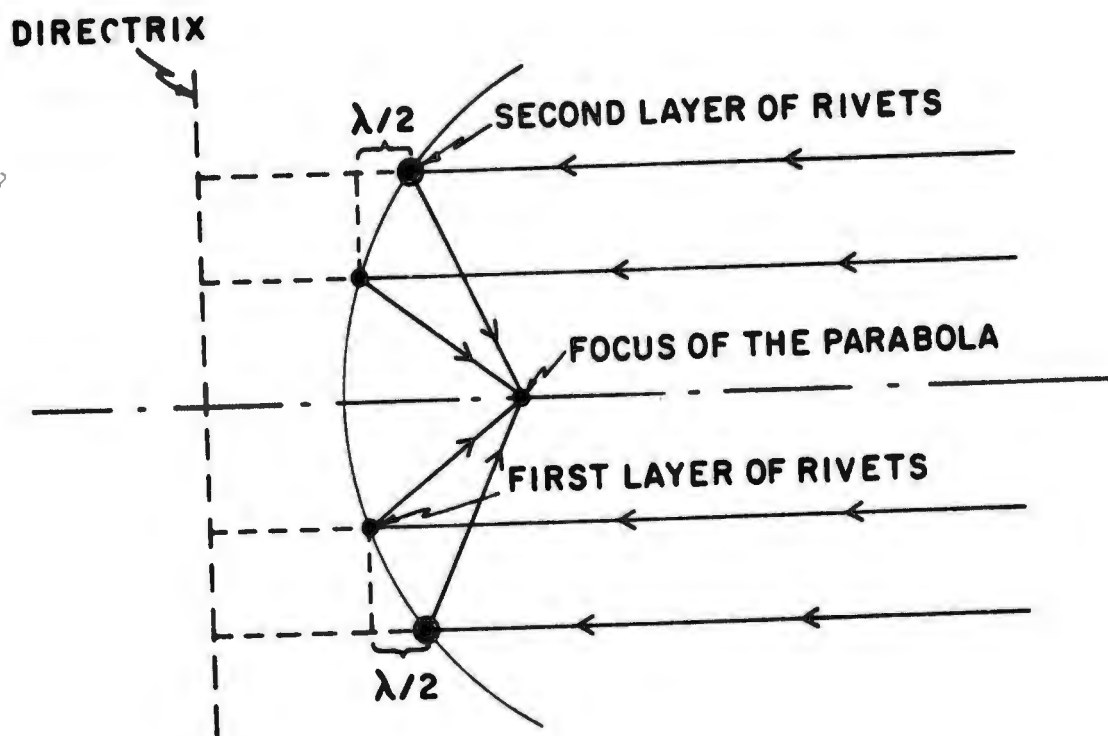


Fig. 11. Possible destructive interference at a certain undesired harmonic frequency for a parabolic reflector.

## 8. CONCLUSION

The mathematical formulation for the analysis of a nonlinearly loaded multiport antenna structure is described and presented. The antenna structure may be situated over a plane imperfect ground. The ground constants could be taken into the analysis, if desired. The formulation is then applied to the analysis of scattering of a 2 element thin-wire antenna array each loaded with a nonlinear load.

Possible cancellation of a specific undesired intermodulation frequency in a certain specific direction where the receiver may be located is demonstrated.

**9. REFERENCES**

- [1] J. J. Bussgang, L. Ehrman, and J. W. Graham, "Analysis of Nonlinear Systems with Multiple Inputs," Proc. IEEE., vol. 62, pp. 1088-1119, August 1974.
- [2] N. Wiener, "Nonlinear Problems in Random Theory," MIT Press, Cambridge, Mass., 1959.
- [3] H. L. Van Trees, "Functional Techniques for the Analysis of the Nonlinear Behavior of Phase-Locked Loops," Proc. IEEE., August 1964, pp. 894-911.
- [4] E. Bedrosian and S. O. Rice, "The Output Properties of Volterra Systems (Nonlinear Systems with Memory) Driven by Harmonic and Gaussian Inputs," Proc. IEEE., 59, December 1971, pp. 1688-1707.
- [5] D. D. Weiner and J. Naditch, "A Scattering Variable Approach to the Volterra Analysis of Nonlinear Systems," Rome Air Development Center, Griffiss Air Force Base, NY, Contract F30602-76-C-0360, Report No. TR-75-11, Syracuse University, Syracuse, NY 13210.
- [6] T. K. Sarkar and D. D. Weiner, "Scattering Analysis of Nonlinearly Loaded Antennas," IEEE Trans. on Antennas and Propagation, March 1976.
- [7] F. M. Tesche, "On the Analysis of Scattering and Antenna Problems Using the Singularity Expansion Technique," IEEE Trans. on Antennas and Propagation, Vol. AP-21, No. 1, January 1973, pp. 53-62.
- [8] H. K. Schuman, "Time Domain Scattering from a Nonlinearly Loaded Wire," IEEE Trans. on Antennas and Propagation, vol. AP-22, No. 4, July 1974.
- [9] R. F. Harrington, "Field Computation by Moment Methods," Macmillan Company, 1963.
- [10] T. K. Sarkar, "An Optimization Program for Linear Arrays of Parallel Wires," IEEE Trans. on Antennas and Propagation, July 1974, pp. 631-632.
- [11] T. K. Sarkar, "Analysis of Radiation by Arrays of Vertical Wire Antennas Over Plane Imperfect Ground (Sommerfeld Formulation); IEEE Trans. on Antennas and Propagation, (to be published).
- [12] T. K. Sarkar, "Analysis of Radiation by Arrays of Horizontal Wire Antennas Over Plane Imperfect Ground (Sommerfeld Formulation) IEEE Trans. on Antennas and Propagation (to be published).
- [13] T. K. Sarkar and B. J. Strait, "Analysis of Arbitrarily Oriented Thin-Wire Antennas Over a Plane Imperfect Ground," Syracuse University Report TR-75, December 1975.
- [14] T. K. Sariam, "Analysis of Radiation by Arrays of Vertical Wire Antennas Over Imperfect Ground (Reflection-Coefficient Method), IEEE Trans. on Antennas and Propagation, vol. AP-23, September 1975, p. 749.

- [15] T. K. Sarkar, "Analysis of Radiation by Arrays of Horizontal Wire Antennas Over Imperfect Ground (Reflection-Coefficient Method)," IEEE Trans. on Antennas and Propagation, (to be published).
- [16] T. K. Sarkar, "Analysis of Radiation by Arrays of Arbitrarily Oriented Wire Antennas Over Plane Imperfect Ground (Reflection-Coefficient Method)," IEEE Trans. on Antennas and Propagation (to be published).
- [17] W. H. Higa, "Spurious Signals Generated by Electron Tunnelling on Large Reflector Antennas," Proc. IEEE, vol. 63, pp. 306-313, February 1975.

Jan 1974

DISTRIBUTION LIST FOR ONR ELECTRONICS PROGRAM OFFICE

Director  
Advanced Research Projects Agency  
Attn: Technical Library  
1400 Wilson Boulevard  
Arlington, Virginia 22209

Office of Naval Research  
Electronics Program Office (Code 427)  
800 North Quincy Street  
Arlington, Virginia 22217

Office of Naval Research  
Code 105  
800 North Quincy Street  
Arlington, Virginia 22217

Naval Research Laboratory  
Department of the Navy  
Attn: Code 2627  
Washington, D. C. 20375

Office of the Director of Defense  
Research and Engineering  
Information Office Library Branch  
The Pentagon  
Washington, D. C. 20301

U. S. Army Research Office  
Box CM, Duke Station  
Durham, North Carolina 27706

Defense Documentation Center  
Cameron Station  
Alexandria, Virginia 22314

Director National Bureau of Standards  
Attn: Technical Library  
Washington, D. C. 20234

Commanding Officer  
Office of Naval Research Branch Office  
536 South Clark Street  
Chicago, Illinois 60605

San Francisco Area Office  
Office of Naval Research  
50 Fell Street  
San Francisco, California 94102

Air Force Office of Scientific Research  
Department of the Air Force  
Washington, D. C. 20333

Commanding Officer  
Office of Naval Research Branch Office  
1030 East Green Street  
Pasadena, California 91101

Commanding Officer  
Office of Naval Research Branch Office  
495 Summer Street  
Boston, Massachusetts 02210

Director  
U. S. Army Engineering Research  
and Development Laboratories  
Fort Belvoir, Virginia 22060  
Attn: Technical Documents Center

ODDR&E Advisory Group on Electron Devices  
201 Varick Street  
New York, New York 10014

New York Area Office  
Office of Naval Research  
207 West 24th Street  
New York, New York 10011

Air Force Weapons Laboratory  
Technical Library  
Kirtland Air Force Base  
Albuquerque, New Mexico 87117

Air Force Avionics Laboratory  
Air Force Systems Command  
Technical Library  
Wright-Patterson Air Force Base  
Dayton, Ohio 45433

**Air Force Cambridge Research Laboratory**

L. G. Hanscom Field  
Technical Library  
Cambridge, Massachusetts 02138

Harry Diamond Laboratories  
Technical Library  
Connecticut Avenue at Van Ness, N. W.  
Washington, D. C. 20438

Naval Air Development Center  
Attn: Technical Library  
Johnsville  
Warminster, Pennsylvania 18974

Naval Weapons Center  
Technical Library (Code 753)  
China Lake, California 93555

Naval Training Device Center  
Technical Library  
Orlando, Florida 22813

Naval Research Laboratory  
Underwater Sound Reference Division  
Technical Library  
P. O. Box 8337  
Orlando, Florida 32806

Navy Underwater Sound Laboratory  
Technical Library  
Fort Trumbull  
New London, Connecticut 06320

Commandant, Marine Corps  
Scientific Advisor (Code AX)  
Washington, D. C. 20380

Naval Ordnance Station  
Technical Library  
Indian Head, Maryland 20640

Naval Ship Engineering Center  
Philadelphia Division  
Technical Library  
Philadelphia, Pennsylvania 19112

Naval Postgraduate School  
Technical Library (Code 0212)  
Monterey, California 93940

Naval Missile Center  
Technical Library (Code 5632.2)  
Point Mugu, California 93010

Naval Ordnance Station  
Technical Library  
Louisville, Kentucky 40214

Naval Oceanographic Office  
Technical Library (Code 1640)  
Suitland, Maryland 20390

Naval Explosive Ordnance Disposal Facility  
Technical Library  
Indian Head, Maryland 20640

Naval Electronics Laboratory Center  
Technical Library  
San Diego, California 92152

Naval Undersea Warfare Center  
Technical Library  
3202 East Foothill Boulevard  
Pasadena, California 91107

Naval Weapons Laboratory  
Technical Library  
Dahlgren, Virginia 22448

Naval Ship Research and Development Center  
Central Library (Code L42 and L43)  
Washington, D. C. 20007

Naval Ordnance Laboratory White Oak  
Technical Library  
Silver Spring, Maryland 20910

Naval Avionics Facility  
Technical Library  
Indianapolis, Indiana 46218